Intrinsic Frequency Response of Silicon–Germanium Phototransistor Associated With 850-nm Multimode Fiber

Zerihun Gedeb Tegegne, Carlos Viana, Jean-Luc Polleux, Marjorie Grzeskowiak, Elodie Richalot

Intrinsic frequency response of Silicon-Germanium phototransistor associated with 850nm multimode fiber

Zerihun Gedeb Tegegne, Carlos Viana, Jean-Luc Polleux, Marjorie Grzeskowiak, and Elodie Richalot

Université Paris-Est, ESYCOM (EA2552), ESIEE-Paris, UPEM, Le CNAM, 93162 Noisy-le-Grand, France

***Abstract*—Theintrinsic frequency response of Silicon-Germanium Heterojunction bipolar Photo-Transistors (HPT) at 850nm is studied to be implemented in multimode fiber systems. The experimental analysis of an HPT with an optical window size of 10x10µm^2 is presented. An Opto-Microwave Scanning Near-Field Optical Microscopy (OM-SNOM) is performed to observe the variation of the HPT dynamic behavior versus the illumination location of the phototransistor. The photocurrent generated by the photodiode at the interface between the n++ sub-collector and the p+ guard ring is analyzed and its impact on the performance of the HPT is investigated. Then, we propose a technique to remove the substrate photocurrent effect on the optical transition frequency (f_{Topt}): the f_{Topt} value of 4.1GHz given by raw measurement results increases up to 6GHz after removing the substrate response. The influence of the two-dimensional carrier flows on the HPT intrinsic Opto-Microwave (OM) behavior is also studied. Design aspects of SiGe/Si HPT structures are finally discussed as a conclusion.**

***Index Terms*— Silicon-based photodetectors, microwave-photonics, SiGe phototransistor, OM-SNOM, Substrate effect**

I. Introduction

An interest has been recently developedin the implementation of SiGe Heterojunction bipolar Phototransistors (HPT) into Radio-over-Fiber (RoF) Home Area Network (HAN)[1][2], for which low cost optoelectronic devices at 850nm are in demand. HPTs can be also specifically used in non-linear circuits such as Direct Optical Injection-Locked Oscillator (DOILO) and self-mixers[3][4]. From 1997 to 2000, Multiple Quantum Well (MQW) SiGe/Si HPT were proposed [5][6]; however, these components are not directly implementable in commercial SiGe BiCMOS technological processes used for electronic parts. Single layer SiGe HPTs have been developed since 2003 [7][8][9][10] based on a standard SiGe HBT technology. Recently, SiGe HPTs were successfully implemented in the transmission chain of 3 Gbps IEEE 802.11.3c signals [1].

Manuscript received January, 2018. This work was partially supported by the French government in the framework of the FUI8 ORIGIN project (Optical-Radio Infrastructure for Gigabit/s Indoor Networks).

Zerihun Gedeb Tegegne, Carlos Viana , Jean-Luc Polleux, Marjorie Grzeskowiak, Elodie Richalot are with the Université Paris Est – ESYCOM laboratory (EA2552), ESIEE Paris, UPEM, Le Cnam, Cité Descartes, BP 99, 93162 Noisy-le-Grand Cedex, France (e-mail: tegegnez@esiee.fr, jl.polleux@esiee.fr).

There is a continuous interest to develop phototransistors from newer standard SiGe HBT technologies that offer faster operating frequencies to improve the performances of the HPTs without modifying the vertical stack of layers imposed by the technological process. To optimize the phototransistor speed, Moutier el al[11]performed physical simulationsto observe the fastest and slowest regions of the HPTs' structure. Other authors [12] and [13]investigated the phototransistor performances through opto-electronic compact circuit modeling. The existence of substrate photocurrent was demonstrated in[13][14][15].

This paper develops amathematical procedure to remove the substrate response and to extract the core performances of SiGe HPT such as the optical transition frequency (f_{Topt}). Concerning these core performances, the intrinsic electrical parameters such as the junction capacitance and transient time are deduced and thenthe influence of the two-dimensional carrier flow (near the metal contacts) on the device speed is demonstrated. A conclusion is then drawn on the design aspects of SiGe/Si HPTs to improve their performances. The measurement of the phototransistor frequency characteristics is performed under multimode optical fiber illumination. While measurement under single mode fiber illumination would bring clear information on the physics of the device, it is also essential to include the impact of the distribution of the multimode fiber optical beam on such characteristics with a view to commercial implementation.

II. SiGe/Si HPT Structure and Technology

The SiGe HPTis fabricated using the conventional SiGe2RF Telefunken GmbH process for bipolar SiGe transistors. Indeed, the phototransistor fabrication respects the vertical stack of layers used in standard SiGe2RF HBT technology. This guarantees the compatibility with this technological process and enables the potential integration of photonic and electronic circuits.

The phototransistor is designed by extending the emitter, base and collector layers of the reference HBT[15]. The optical injection is made vertically through the emitter. A cross-section of the phototransistor structure is given in Figure 1. The light path goes through the oxide and polysilicon of the emitter before entering the Si emitter, SiGe base and Si collector regions. This HPT is essentially one large HBT whose emitter metallization only partially covers the emitter

region. The substrate is grounded through a p+ guard ring around the HPT.

We have designed phototransistors with a 10x10 µm^2 optical opening. The base region consists of a 40-80 nm thin SiGe layer with Ge content of 20-25 % and high p doping in the range of 10^{19} cm^{-3} as presented in [6].The collector is typically 300-400 nm thick with low doping and the emitter region is less than 100nm thick. The doping levels of each region are estimated in[16].

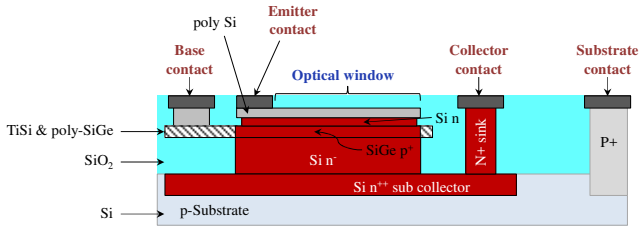

Figure 1: Simplified schematic cross-section of HPT with extended Emitter, Base and Collector regions.

III. Experimental Results and Discussion

A. *Substrate photodiode current analysis*

The Gummel plots under illumination (at 850 nm wavelength) and dark conditions are shown inFigure 2. The current at low base-emitter voltage (Vbe) corresponds to the photocurrent which is far lower than the current induced by the transistor effect observed at higher base-emitter voltage. Under illumination condition, the base current in Figure 2is represented by its absolute value. At low Vbe, the base current Ib has a negative sign and hence flows out of the base contact.Its sign changes at Vbe=0.82 V where its amplitude is minimal.

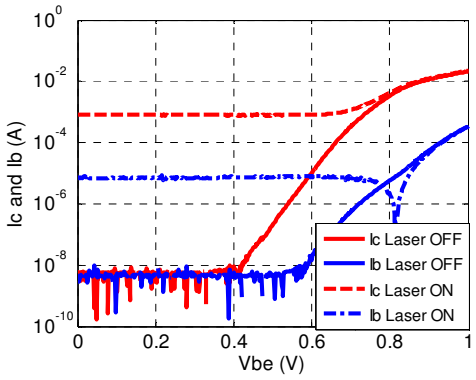

Figure 2: Gummel plot under 2.28 mW optical power illumination and dark conditions.

Under dark condition and at low Vbe, the magnitude of the collector current Ic and the base current Ib are equal, whereas for the same biasing condition with the light "ON", the magnitude of Ic and Ib are different. This behavior is not encountered with phototransistors such as InGaAs/InP HPTs[17] (for which the magnitude of Ib and Ic are equal at low base-emitter voltage and under illumination condition)where the InP substrate is optically transparent at the wavelength of interest. As it is indicated in Figure 3, the holes (h+) generated in the substrate diode is effetely grounded via the substrate contact. However, the electrons (e-) generated in the substrate diode is combined with theelectrons which are generated in the active region (emitter-base-collector) of the HPT toreached the collector contact and measured as collector current, I_C. When Vbe is greater than 0.7V, most parts of the holes generated at the base-collector junction attract electrons from the emitter for transistor amplification and some parts are however escaped to the base contact. Whereas, when Vbe less than 0.4V, all photo-generated holesgenerated within the active regionis flowing out into the base contact and can be measured as base current, Ib.Thus, the difference between collector and base photocurrent magnitudes shown in Figure 2at Vbe=0V corresponds to the photocurrent generated by the substrate diode called substrate photocurrent (I_{sub})[14]. This can be computed using the equation below:

$$I_{sub} = \left(I_{C,PD} - I_{C,PD,dark}\right) - \left(I_{b\_PD} - I_{b\_PD\_dark}\right) \quad (1)$$

where $I_{b\_PD\_dark}$ and $I_{C,PD,dark}$ are respectively the dark base and collector currents in photodiode (PD) mode (at Vbe=0V). $I_{C,PD}$ and $I_{b,PD}$ are the collector and base currents under illumination condition.

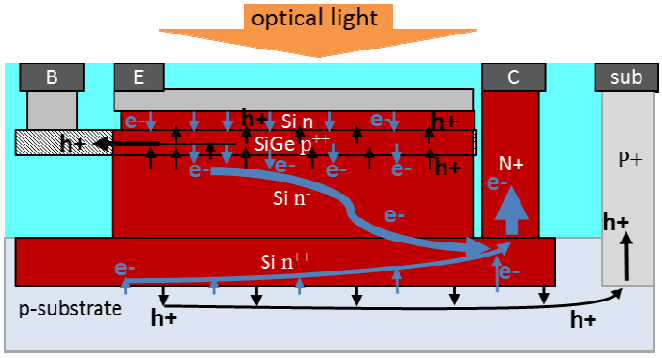

Figure 3: the schematic that indicates the flow of photo-generated carriers that are generated at different region of the HPT.

To locate the source of this extra photocurrent in the phototransistor structure and to study its impact on the Opto-Microwave (OM) behavior of the HPT, we performed a DC and an opto-microwave mapping of the devicesusing Scanning Near Field Optical Microscopy (SNOM) with the measurement setup described in[18][19],where a 850 nm VCSEL (of 12GHz cutoff frequency) is directly modulated to illuminate the HPT through a lensed Multi-Mode Fiber (MMF)moved over the HPT surface.

Figure 4-a) shows the microscopic photography of the 10x10 µm² phototransistor (over which the topological mapping is performed) where the ground (emitter contact) and signal (base and collector) lines are clearly visible. The base contact is taken from the left side, collector contact from the right side and the emitter contact is connected at its top and bottom sides to the ground (common emitter configuration).

The layout is accordingly sketched in Figure 4-b) which defines the coordinates of the optical fiber center; its origin is fixed at the center of the optical window.

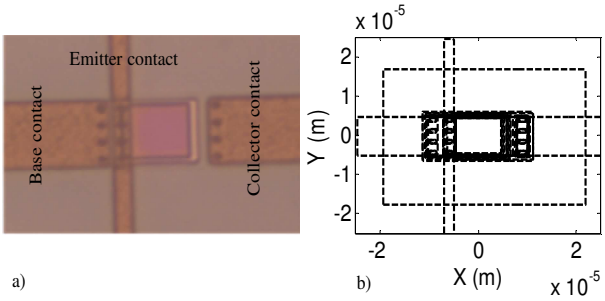

Figure 4: a) Top view of the phototransistor; b) Layout of the 10x10 µm² optical window phototransistor and optical fiber coordinate axes centered at the center of optical window.

We performed the experimental mapping (consisting of displacing the illuminating optical fiber) on HPT at two different bias conditions i.e. at Vbe=0V and Vbe=0.857V for Vce=3V. The phototransistor mode (HPT mode) is obtained by fixing the collector-emitter voltage at 3 V and a fixed base-emitter voltage at 0.857 V. These biasing conditions correspond to the optimal ones in terms of opto-microwave responsivity. In this mode, there is an internal amplification of photo-generated carriers due to transistor effect (current gain β). The photodiode mode (PD mode) is obtained by setting the collector-emitter voltage at 3 V and the base-emitter voltage at 0 V. In PD mode, as the base-emitter junction is electrically inactive, there is no amplification in the deviceso that the purely photo-generated currents can be extracted. The DC current and opto-microwave frequency response of the HPT is then measured at each location of the illuminating optical beam in both modes.An injected optical power level of 2.38mW is used in the subsequent experimental results.

B. Substrate photocurrent effect on opto-microwave behavior

The opto-microwave (OM) power gain represents the ratio of the HPT microwave output signal power to the output power of a photodiode with 1A/W responsivity [5]. It is equal to the square of the responsivity under 50Ω load condition but may change as a function of the load as described in depth in[20].OM gain is extracted from S-parameter measurement as a function of frequency. Figure 5-a) and -b) show the low frequency (50 MHz) OM responsivity of a 10x10 µm² optical window size HPT (loaded by 50 Ω) as a function of the optical fiber position in HPT and PD modes, respectively. In HPT mode, the peak of the responsivity appears inside the optical window, whereas in PD mode, the responsivity is maximal when the optical fiber is around the optical window according to a ring shape as shown in Figure 5-b).

The ring shape of the maximal responsivity in PD mode is due to the illumination of the substrate diode; we can observe the responsivity of the substrate diode is clearly stronger than the one of the photodiode created by the base and collector in the active region. As shown in Figure 5-a) the ring shape does not appear in phototransistor mode as the substrate diode effect is hidden by the transistor amplification.

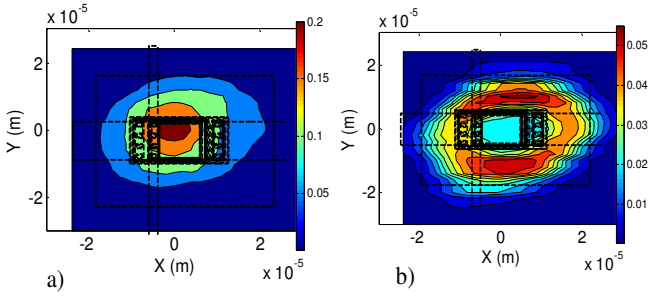

Figure 5: Low frequency (50 MHz) opto-microwave responsivity of HPT with 10x10 µm² in a) HPT mode (Vbe=0.857 V), b) PD mode (Vbe=0 V) for Vce=3 V loaded by 50 Ω.

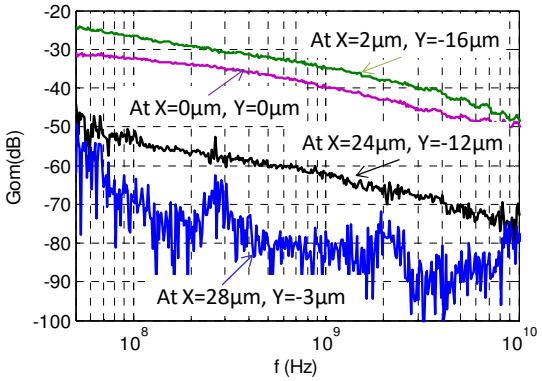

Figure 6: Gom as a function of frequency in photodiode mode at different positions of optical fiber extracted from figure 9-b).

Figure 6presents the OM gain (Gom)as a function of the frequency at different optical fiber locations extracted from Figure 5-b) (in photodiode mode). The Gom at X=2 µm and Y= –16 µm (outside the optical window) is higher than the Gom at the center (X=Y=0 µm) at all frequencies. From this result, we can deduce that the substrate diode is clearly dominating over the intrinsic diode (the diode created by the base and collector) even at the central position despite the optical beam is attenuated by the layer vertical stack. When the optical fiber moves further away from the optical window, the low frequency Gom decreases until reaching the noise level as the substrate diode becomes slower and then non effective to detect the 50 MHz signal. The Gom curves at (X=24 µm, Y= –12 µm) and (X=28 µm, Y= –3 µm) illustrate this evolution in Figure 6.

The substrate responsivity can be isolated from the intrinsic behavior by the mathematical model as described in the following section. The photodiode mode intrinsic responsivity ($R_{PD,i}$), substrate responsivity (R_{sub}) and raw responsivity ($R_{om,PD}$) for an illuminated beam displacing along Y axis(X=0) are presented in Figure 7. Indeed, the $R_{om,PD}$ curve corresponds to the variation along the line X=0 of the PD mode responsivity measured at 50 MHz and presented in Figure 5-b. To extract the substrate responsivity at 50 MHz we use the definition of OM power gain in[7], and considering the 50 Ω load, it comes:

$$G_{om} = \frac{\frac{1}{2}R_0\left(I_{c,PD}\right)^2}{\frac{1}{2}R_0\left(I_{opt,\mathrm{RF}}\right)^2} = R_{om,PD}{}^2 \Rightarrow with I_{opt,\mathrm{RF}} = \alpha_{cal} P_{opt,\mathrm{RF}} \quad (2)$$

and

$$I_{C,\mathrm{PD}} = I_{C,\mathrm{PD},ph} + I_{C,\mathrm{PD,dark}} + I_{sub} \quad (3)$$

where $I_{C,PD}$is the total current measured at the collector contact in PD mode, $I_{C,PD,ph}$is the photocurrent generated in the HPT active area in PD mode, $I_{C,PD,dark}$ is the dark current measured at the collector contact, I_{sub} is the substrate photocurrent, $R_{om,PD}$ is the raw OM responsivity in PD mode, α_{cal} is a 1 A/W normalization factor and $P_{opt,RF}$ is the illuminating optical power expressed as the equivalent current $I_{opt,RF}$. Then we deduce the intrinsic responsivity:

$$R_{PD,i}{}^2 = \left(\frac{I_{C,\mathrm{PD},ph}}{I_{opt,RF}}\right)^2 = \left(\frac{I_{C,\mathrm{PD}} - I_{C,\mathrm{PD,dark}} - I_{sub}}{I_{opt,RF}}\right)^2 = \left(R_{om,PD} - R_{sub}\right)^2 \quad (4)$$

$$R_{PD,i} = \frac{I_{C,\mathrm{PD}} - I_{C,\mathrm{PD,dark}}}{I_{opt,RF}} - \frac{I_{sub}}{I_{opt,RF}} = R_{om,PD} - R_{sub} \quad (5)$$

To extract the substrate responsivity (R_{sub}) at low frequency, we assume that the intrinsic DC responsivity ($R_{PD,\ i,\ DC}$) is equal to the intrinsic responsivity at low frequency ($R_{PD,i,LF}$), this assumption being valid for Vce=3 V with no amplitude variation atlow frequency. Hence:

$$R_{PD,i,\mathrm{LF}} = \frac{I_{C,\mathrm{PD},ph}}{I_{opt,RF}} \cong \frac{I_{C,\mathrm{PD},ph}}{I_{opt,\mathrm{DC}}} = R_{PD,i,DC} \quad (6)$$

Thus the substrate responsivity (R_{sub}) at low frequency is calculated from equation (5) and (6).

$$R_{sub} = R_{om,PD} - R_{PD,i,LF} \quad (7)$$

As presented in Figure 7, the peak of intrinsic responsivity ($R_{PD,\ i,\ DC}$)appears at the center of the optical window (X=Y=0 µm) whereas at the same location the substrate photodiode responsivity is weaker than the intrinsic photodiode responsivity.However, the substrate response becomes stronger when the optical beam moves outside the optical window (around Y=±10 µm). The substrate responsivity is low in the HPT's active region, but it is not null due to the optical light penetration through the HPT to the substrate, underneath the active region.

The dynamic behavior of the phototransistor can be analyzed through the optical transition frequency (f_{Topt}). The latter is defined as the frequency at which the 50 Ω OM gain in HPT mode is equal to the 50 Ω low frequency gain in PD mode (Vbe=0 V). Indeed, it is the frequency at which the phototransistor stops amplifying as shown in Figure 9.

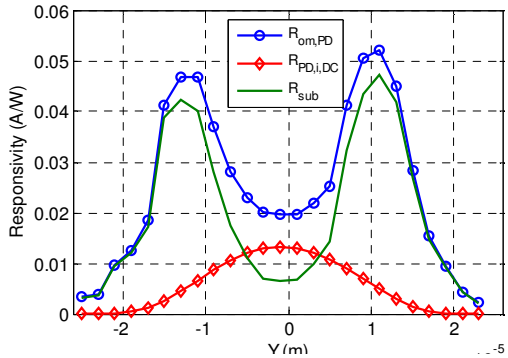

Figure 7: The raw ($R_{om,PD}$), substrate (R_{sub}) and intrinsic responsivity ($R_{PD,\ i,\ DC}$) of HPT with 10x10 µm^{2}optical window size in PD mode operation (Vbe=0 V) and for an optical beam along Y axis (X=0) axis.

As it has been demonstrated in [14], the substrate photocurrent in SiGe HPT has a huge impact on the frequency response of the phototransistor mainly in PD mode. To observe the intrinsic properties of the HPT (that can be used for future SiGe HPT modeling), one needs to remove (de-embed) the substrate response from the raw measured data at each position of the optical fiber and atallfrequencies. The substrate response at low frequency computed by equation (7) is extrapolated to all frequencies using the transfer function presented in equation (8).

$$R_{sub}(f) = \frac{R_{sub}(\mathrm{f}_0)}{\left(1 + j\frac{f}{\mathrm{f}_0}\right)^{\alpha}} \quad (8)$$

wheref_0 is 50 MHz and $\propto$ is the order of the transfer function to model the frequency slope of the substrate photodiode.

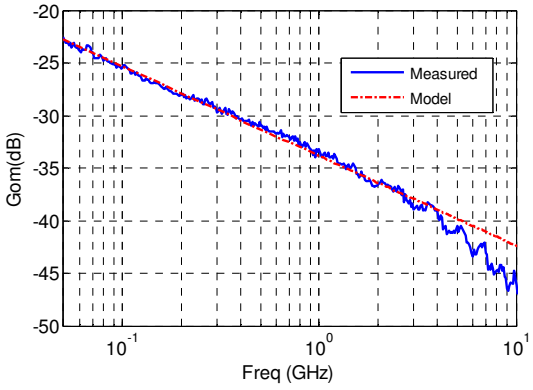

Figure 8: The transfer function model fitted to the measured OM gain of the substrate photodiode (optical fiber located at *X*=5 µm, *Y*=15 µm and biases Vbe=0 V, Vce=3 V).The level of the injected optical power is 2.38mW.

Figure 8 shows the fitting of the model with the experimental OM gain measured by illuminating the structure at X=5 µm and Y=15 µm where the substrate photocurrent amplitude is maximum. The model well fits with the measurement results for ∝=0.4 corresponding to an

8 dB/decay slope of Gom.

The substrate diode influence is then removed at all frequencies from the phototransistor responsivity to obtain the intrinsic responsivity in phototransistor mode ($R_{HPT,i}$). The intrinsic optical transition frequency ($f_{Topt,int}$) is the frequency at which $R_{HPT,i}$ is equal to the intrinsic DC responsivity in photodiode mode ($R_{PD,i,DC}$).

The complete and intrinsic OM gains versus frequency in PD and HPT modes when the optical beam focuses at the center of the optical window (X=0 µm, Y=0 µm) is presented inFigure 9. The model of substrate photodiode frequency response at X=Y=0 µm is also presented in the same figure. The raw and intrinsic Gom are equal at all frequencies in HPT mode operation. This indicates that the frequency response of the substrate photodiode is hidden by the internal transistor amplification effect. However, in PD mode, the substrate photodiode contributes to its OM gain and reduces its speed.

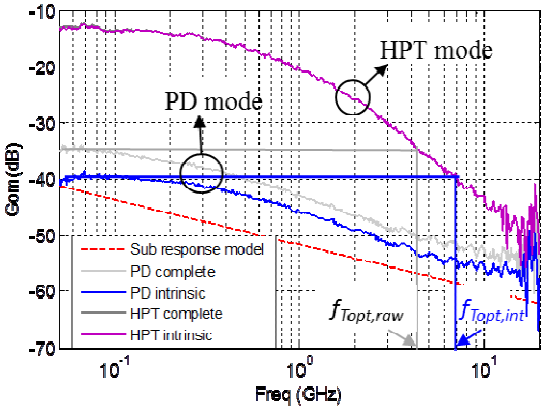

Figure 9: OM gain in photodiode and phototransistor modes for an optical beam located at *X*=0 µm and *Y*=0 µm.The level of the injected optical power is 2.38mW.

The variation of f_{Topt} at X=0 µm along Y-axis is shown in Figure 10-a) before and after removing the substrate diode effect. The a flat $f_{Topt,int}$ peak appears over the optical window (the peak width is about 10 µm), anditdrops to zero outside the optical window.

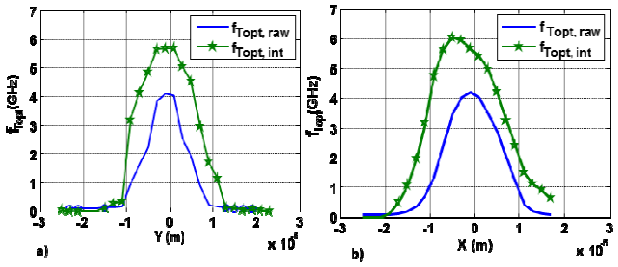

Figure 10: Optical transition frequency before and after removing the substrate diode effect with the optical beam centered at X=0 µm (a) and Y=0 µm (b).

Whereas, along X- axis, the intrinsic $f_{Topt,int}$ is not flat over the optical window (Figure 10-b). The intrinsic $f_{Topt,int}$ peak is shifted from the center of the optical window towards the base and emitter contacts. This is because when the optical beam is injected close to the base and emitter contacts, the distance travelled by the holes to reach the base and emitter contacts become very short, whereas when the optical beam is injected at the center of the optical window, the distance travelled by the holes to reach the base and emitter contacts is longer as the related transit time. The f_{Topt} peak is improved from 4.1 GHz to 6 GHz while extracting substrate diode effect.

Figure 11 shows the intrinsic optical transition frequencies $f_{Topt,int}$ versus collector current (I_C). The presented optical transition frequency has been measured after optimizing the optical fiber location to obtain the higher $f_{Topt,int}$. The maximal value of $f_{Topt,int}$ reaches 6.5 GHz, indicating that this HPT could be implemented in optical applications operating up to 6.5 GHz.

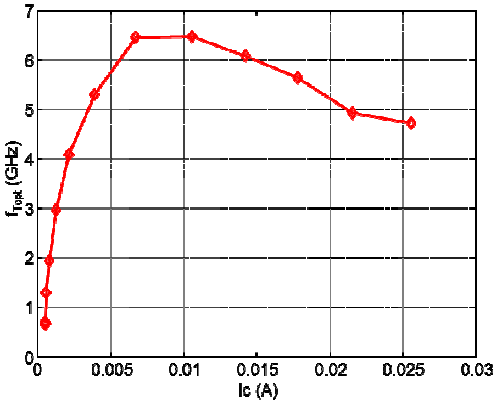

Figure 11*:* The optical transition frequency f_{Topt}as a function of the collector current.The injected optical power is 2.38mW.

The f_{Topt} versus I_C curve (Figure 11) can be divided into three mean regions:

1) *Low current region:*
   In this region f_{Topt} quickly increases with the collector current due to the junction capacitance reduction as the dc supply increases.
2) *Medium current region:*
   The peak of f_{Topt} is reached between I_C=6 mA and 12 mA. The frequency behavior in this region is mainly limited by the carrier time to reach the metal contacts. Photo-generated carrier transit time is the main limiting factors of the peak f_{Topt}.
3) *High injection current region:*
   For I_C greater than 12 mA, f_{Topt} quickly drops, due to the injection of a large number of carriers (*Kirk effect)* in the device which limits the speed of HPTs.

The peak value of the f_{Topt} (6.5GHz) is very small compared to its equivalent electrical transition frequency (f_T = 47.3GHz) as shown in Figure 12. Unlike f_T, f_{Topt} is influenced by additional terms related to the photo-detection mechanism such as additional transit time and junction capacitances introduced by the injected optical power.

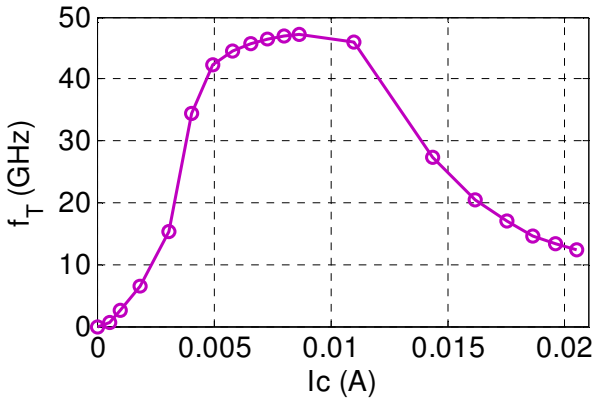

Figure 12: The electrical transition frequency f_T as a function of the collector current.

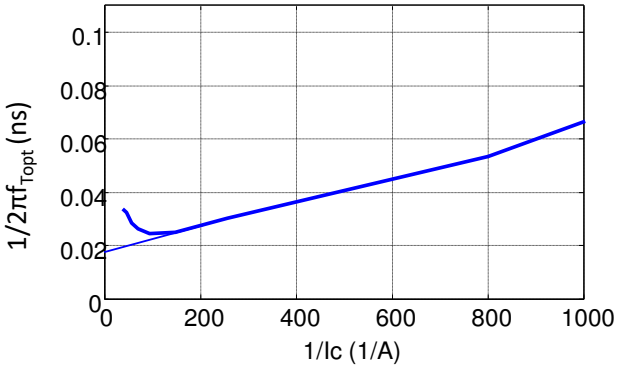

Figure 13: The opto-microwave transit time delay versus 1/Ic to extract the junction capacitances from the curve slop and the opto-microwave transit time from y-intercept.

The intrinsic parameters of the HPT such as the capacitances and transit time can also be deduced experimentally from optical transition frequency. These parameters could be used in optical system modeling to implement the HPT as a photodetector as well as for future study of the HPT structures. The opto-microwave transition time delay τ_{F_OM} is the time required by the opto-microwave photo-generated carriers to reach any contact and is calculated from f_{Topt} according to $\tau_{F\_OM}=1/(2\pi f_{Topt})$ [19]. Figure 13 shows the opto-microwave transition delay versus $1/I_C$. The totalcapacitance (including base-emitter and base-collector depletion, diffusion and parasitic)and the transit time of the phototransistor can be extracted from the slope and y-intercept of the transition time delay curve respectively. Table 1 compares the extracted electrical (τ_F, C_E), opto-microwave (τ_{F_OM}, C_{OM}) and optical (τ_{F_opt}, C_{opt}) transit times with the related capacitances. The first two parameters (electrical and opto-microwave) are extracted from $f_T$and f_{Topt} respectively. The optical terms are deduced by removing the electrical terms from the opto-microwave ones.

Table 1: The extracted junction capacitances and forward transit times of the HPT illuminated at the position corresponding to the optimal f_{Topt}.

Electrical		**Total(Opto-microwave)**		**Optical**	
C_E(pF)	τ_F(ps)	C_{OM} (pF)	τ_{F_OM} (ps)	C_{opt} (pF)	τ_{F_opt} (ps)
0.798	1.5	1.7	18.7	0.902	17.2

Larger values of capacitance and transit time under opto-microwave operation mean that photo-generated carriers cover a longer path than the electrically generated ones. Indeed, the active region of the electrical transistor corresponds to the vertical region of the emitter contact, whereas the transistor effect (active area of the HPT) under opto-microwave operation is distributed along the whole device with additional lateral paths of photo-carriers to reach the electrical contacts. Similarly, capacitance is larger under opto-microwave operation, when compared with under electrical operation, as the active surface of the structure increases related to the photo-detection process. Thisimplies both the junction and diffusion capacitancesincrease related to the injected optical power.

We deduce the “optical” capacitance and transit time by removing the electrical parameters from the opto-microwave ones. These values correspond to the additional capacitance and transit time due to the additional path length and the equivalent active surface area increase encountered by photo-generated carriers compared to the electrical ones. “Optical” capacitance is higher than the half of the total opto-microwave one. Such variation of the equivalent capacitance may correspond to a corresponding double surface. Optical transit time is much larger than the electrical one. Considering that the vertical stack is unchanged, this may be attributed to a lateral path required for holes to be amplified or for electrons injected from the emitter to reach the photo-generated holes in the base region.

IV. Conclusion

This paper considered a SiGe/Si phototransistor developed by using the industrial SiGe HBT technology without modifying the vertical stack of layers. The OM SNOM analyse is shown to be crucial to understand the behavior of such SiGe HPTs. It allows the extraction of the DC and dynamic behaviors of the device for all the positions of the illuminating optical fiber. As slow carriers from the substrate diode affect the dynamic response of the SiGe/Si HPTs, an extraction method has then been developed to isolate the substrate effect and then deduce the intrinsic behavior of the HPT; an intrinsic optical transition frequency of 6 GHz has been obtained. Thus, the impact of the two dimensional carriers flow in the intrinsic phototransistor structure is demonstrated. The speed increases when we illuminate the HPT close to the base contact and it gradually decreases when the optical beam moves away from the base-emitter contact. This is due to the speed of holes which are collected at the base-emitter region.

The internal electrical parameters such as transit time and capacitances of the phototransistor are extracted and can be an input for future modeling of the phototransistor. Further studies using a single mode optical fiber would be interesting for a more precise modeling of the SiGe HPT and for a reduction of the substrate diode effect when illuminating the optical window.

Several alternatives exist to eliminate the substrate contribution, as the design of metallic diaphragms around the optical window to hide the substrate photodiode, or through lateral illumination of the HPT. Alternatively, taking advantage of the substrate effect could be envisaged for a combined HPT-PD structure.The influence of the 2D carriers flow effect can also be avoided or minimized via a proper designof the metal contacts to get a symmetric contact of the collector, base and emitters that will make the electrical field more vertical.

V. ACKNOWLEDGEMENT

This work was partly supportedby the French DGCIS FUI8 ORIGIN project.

REFERENCES

[1] C. Viana, Z.G. Tegegne, M. Rosales, J.L. Polleux, C. Algani, V. Lecocq, C. Lyszyk and S. Denet “Hybrid photo-receiver based on SiGe heterojunction photo-transistor for low-cost 60 GHz intermediate-frequency radio-over-fibre applications” IEEE electronic letters, Vol. 51, No.8, pp640-642, April2015.

[2] J. Guillory, A. Pizzinat, B. Charbonnier and C. Algani “60GHz Intermediate Frequency over Fiber using a passive Multipoint-to-Multipoint architecture”, IEEE NOC, pp44-47,Newcastle-Upon-Tyne, UK,July 2011.

[3] Kwang-Hyun Lee, Jae-Young Kim, Woo-Young Choi, Hideki Kamitsuna, Minoru Ida, and Kenji Kurishima “Low-Cost Optoelectronic Self-Injection-Locked Oscillators” IEEE Photonics Technology Letters, Vol. 20, No. 13, July 1, 2008.

[4] Hideki Kamitsuna, Tsugumichi Shibata, Kenji Kurishima, and Minoru Ida“Characteristics of InP–InGaAs HPT-Based Optically Injection-Locked Self-Oscillating Optoelectronic Mixers and Their Influence on Radio-Over-Fiber System Performance” IEEE Photonics Technology Letters, Vol. 19, No. 3, February 1, 2007.

[5] Y. Zhu, Q. Yang, Q. Wang “Resonant Cavity SiGe/Si MQW Heterojunction Phototransistor Grown on the SIMOX Substrate for 1.3pm Operation” Electronic Components and Technology Conference, San Jose, CA, USA, pp.1199-1204, May1997.

[6] Z. Pei, C. S. Liang, L. S. Lai, Y. T. Tseng, Y. M. Hsu, P. S. Chen, S. C. Lu, M.-J. Tsai, and C. W. Liu, “A High-Performance SiGe–Si Multiple-Quantum-Well Heterojunction Phototransistor” IEEE electronic letters, Vol. 24,No.10, pp643-645, September 2003.

[7] J.L. Polleux, F. Moutier, A.L. Billabert, C. Rumelhard, E. Snmez, H. Schumacher, “A Strained SiGe layer Heterojunction BipolarPhototransistor for Short-Range Opto-Microwave Applications” in IEEE- MWP2003, Budapest, Hungary, pp113-116, September 2003, .

[8] M. D. Rosales, J. Schiellein, C. Viana, J.-L. Polleux, and C. Algani, “Full area emitter SiGe phototransistor for opto-microwave circuit applications,” in Proc. 9th IEEE Int. Conf. Group IV Photon, San Diego, CA, USA, Aug. 2012, pp. 294–296

[9] Z. Pei, J. W. Shi, Y. M. Hsu, F. Yuan, C. S. Liang, C. Lu, W. Y. Hsieh, M. J. Tsai, W. Liu, “Bandwidth Enhancement in an Integratable SiGe Phototransistor by Removal of Excess Carriers”, IEEE Electron Device Letters, Vol. 25, No.5, pp286-288, May 2004.

[10] T. Yin, A.M. Pappu, A.B. Apsel “Low-cost, high efficiency and high-speed SiGe phototransistors in commercial BiCMOS”. IEEE Photonics Technol. Lett., Vol. 18, No. 1,pp.55-57, December 2006.

[11] F. Moutier, J.L. Polleux, C. Rumelhard, H. Schumacher, “Frequency response enhancement of a single strained layer SiGe phototransistor based on physical simulations”. GAAS Conf. of the European Microwave Week, pp.113-116, Paris, France, May 2005.

[12] Helme.J.P, Houstron.P.A “Analytical modeling of speed response of heterojunction bipolar phototransistors”. Lightwave Technology. Vol. 25, No.5, pp. 1247-1255, April 2007.

[13] F. Yuan, J. W. Shi, Z. Pei, C. W. Liu “MEXTRAM modeling of Si-SiGe HPTs”. IEEE Trans. Electron Devices, Vol. 51, No. 6, pp. 870-876, May 2004.

[14] Z. G. Tegegne, C. Viana, M. Rosales, J.-L. Polleux, C. Algani, M. Grzeskowiak, E. Richalot, "Substrate diode effect on the performance of Silicon Germanium phototransistors", in IEEE MWP, pp.1-4, Paphos, Cyprus, October2015.

[15] J.-W. Shi, Z. Pei, F. Yuan, Y.-M. Hsu, C.-W. Liu, S. C. Lu, and M.-J. Tsai, “Performance enhancement of high-speed SiGe based heterojunction phototransistor with substrate terminal” Appl. Phys. Lett., Vol. 85, No.14, October 2004, dio: 10.1063/1.1799237

[16] J.L. Polleux, F. Moutier, A.L. Billabert, C. Rumelhard, E. Sönmez2, H. Schumacher “An SiGe/Si Heterojunction Phototransistor for Opto-Microwave Applications: Modeling and first Experimental Results” 11th GAAS2003 symposium, 6-10 October 2003, Munich

[17] J. Schiellein, M. Rosales, J.L. Polleux, C. Algani, T. Merlet, M. Riet, J. Godin, and A. Scavennec, “Analysis of opto-microwave paths into a InP/InGaAs UTC-HPT,” IEEE *Microwave Conference (EuMC),* pp. 949 –952,Manchester, UK,Oct. 2011

[18] Z. G. Tegegne, C. Viana, M. Rosales, J. Scheillein, J.L. Polleux, C. Algani, M. Grzeskowiak and R. Elodie, “An 850nm SiGe/Si HPT with a 4.1GHz maximum Optical Transition Frequency and 0.805A/W Responsivity”, in International journal of microwave and wireless technologies, Vol. 9, Issue 1, pp.17-24, February 2017.

[19] Zerihun.G. Tegegne "SiGe/Si Microwave Photonic Phototransistors and Interconnects towards Silicon-based full Optical Links", Ph.D. thesis, Université Paris-Est, ESYCOM- ESIEE Paris, May 2016.

[20] Jean-Luc Polleux, Laurent Paszkiewicz, Anne-Laure Billabert, Jacques Salset, and Christian Rumelhard, “Optimization of InP–InGaAs HPT Gain: Design of an Opto-Microwave Monolithic Amplifier” IEEE Transactions On Microwave Theory And Techniques, Vol. 52, No. 3, March 2004.